Concrete for Pavements. HRB, Bull. 332, 1962, pp. 40-94.
8. S. Nagataki. Shrinkage and Shrinkage Restraints in Concrete Pavements. Journal of the Structural Division, ASCE, July 1970.
9. J.W. Murdock. A Critical Review of Research on Fatigue of Plain Concrete. Engineering Experiment Station, Univ. of Illinois, Urbana, Bull. 475, 1965.
10. Thickness Design for Concrete Pavements. Portland Cement Association, Skokie, IL, 1966.
11. M.I. Darter and E.J. Barenberg. Design of Zero Maintenance Plain Jointed Concrete Pavement: Vol. II, Design Manual. FHWA, Rept. FHWA-RD-77-112, June 1977.
12. J.H. Swanberg. Temperature Variation in a Concrete Pavement and the Underlying Subgrade. HRB, Proc., Vol. 25, 1945, pp. 69-180.
13. B.M. Maguire, M.A. Sozen, and C.P. Siess. A Study of Stress Relaxation in Prestressing Reinforcement. Journal of the Portland Cement Association, April 1964, pp. 13-57.
14. A.N. Hanna, P.J. Nussbaum, T. Arriyavat, J. Tseng, and B.F. Friberg; Portland Cement Association. Technological Review of Prestressed Pavements. FHWA, Rept. FHWA-RD-77-8, Dec. 1976.
15. E.F. Kelley. Structural Design of Concrete Pavement. Journal of the American Concrete Institute, Vol. 35, Supplement, Sept. 1939.
16. G.S. Paxson. Investigational Concrete Pavement in Oregon. HRB, Res. Rept. 3B, 1945, pp. 77-89.
17. R.W. Carlson. Drying Shrinkage of Large Concrete Members. Journal of the American Concrete Institute, Jan.-Feb. 1937, pp. 327-336.
18. G.E. Troxell, J.M. Raphael, and R.E. Davis. Long-Time Creep and Shrinkage Tests of Plain and Reinforced Concrete. Proc., ASTM, Vol. 58, 1958, pp. 1101-1120.
19. W.R. Lorman. The Theory of Concrete Creep. Proc., ASTM, Vol. 40, 1940, pp. 1082-1102.
20. A.M. Neville. Properties of Concrete. Pitman Publishing, Ltd., London, 1981.
21. G.S. Paxson. Report on Experimental Project in Oregon. HRB, Res. Rept. 17B, 1956, pp. 151-155.
22. E.C. Sutherland. Analysis of Data from State Reports. HRB, Res. Rept. 17B, 1965, pp. 1-11.
23. Joint-Related Distress in PCC Pavement: Cause, Prevention, and Rehabilitation. NCHRP, Synthesis of Highway Practice 56, 1979.
24. G.E. Albritton. Prestressed Concrete Highway Pavement: Performance During Construction. Paper presented at 57th Annual Meeting, Transportation Research Board, Washington, DC, Jan. 1978.
25. G.R. Morris and H.C. Emery. The Design and Construction of Arizona's Prestressed Concrete Pavement. Research Section, Highway Division, Arizona Department of Transportation, Phoenix, Jan. 1978.
26. P.J. Nussbaum, S.D. Tayabji, and A.T. Ciolko. Prestressed Pavement Joint Design. FHWA, June 1981.
27. G.R. Morris. Full-Depth, Full-Width Designs and Prestressed Concrete Pave the Way for Arizona's Highways. Civil Engineering, ASCE, March 1978.

Publication of this paper sponsored by Committee on Rigid Pavement Design.

Comparison of Solutions for Stresses in Plain Jointed Portland Cement Concrete Pavements

D. R. MacLEOD AND C. L. MONISMITH

A number of existing models to compute the stresses in plain jointed portland cement concrete (PCC) pavements due to traffic loads are examined, and those that show the most promise are recommended. Solutions examined include (a) plate on dense-liquid subgrades, closed form and finite elements; (b) plate on elastic solid, closed form and finite element; and (c) layered elastic system, closed form and finite element (two-dimensional and three-dimensional representations). Although the three-dimensional finite-element analysis for the layered elastic solid is probably the most representative of the methods examined, the associated computer costs preclude its use on a routine basis at this time. The study does show that a two-dimensional finite-element analysis for the same representation is suitable for determining load-associated stresses in plain jointed PCC pavements. Changes in the engineering properties of materials, climate variations, and loading conditions can be accommodated. The maximum tensile stress—the controlling factor in the fatigue life of PCC pavements—occurs near the edge of the PCC at the midslab position. A finite-element analysis, which allows for the consideration of the strengths of the cement-stabilized layer (not accounted for in a dense-liquid subgrade type of analysis), has demonstrated that the stiffness of the cement-stabilized layer has an important effect on the fatigue life of PCC pavements. This analysis has indicated that different cracking-behavior patterns can be identified with different stabilized layer stiffnesses. A detailed traffic analysis, with allowances for thermal stresses and material variabilities, has indicated that there is a common fatigue relation for PCC pavements when the failure criteria $N_f = 225\,000\,(MR/\sigma)^4$ is used.

It has long been recognized that cracking in portland cement concrete (PCC) pavements cannot be related to traffic alone, but such factors as climate, pavement material stiffnesses, strengths, and thicknesses are significant in establishing pavement behavior as well. To date, mechanistic models have not been able to deal satisfactorily with these factors. This paper examines some of the existing models that have been used to analyze the development of load-associated cracking in plain jointed PCC pavements. Based on these analyses, those representations that have promise are recommended for use, recognizing that a satisfactory predictive model for PCC pavement cracking should

1. Predict the location, type, and severity of distress;
2. Be adaptable to various climatic conditions;
3. Allow for changes in the engineering properties of materials (in particular, the model should realistically reflect the influence of various stabilized subbases on performance);
4. Allow for changes in loading conditions (this

Table 1. Transverse and longitudinal first-stage cracking patterns for pavements with 8-in concrete layers, San Francisco Bay area.

Route No.	Transverse Cracking (%)	Longitudinal Cracking (%)
CTS designs		
US-101, Marin and Sonoma Counties	97	3
I-80, Alameda and Contra Costa Counties	90	10
CA-17, Santa Clara and Alameda Counties	84	16
CTB designs		
US-101, Marin and Sonoma Counties	40	60
I-680, Alameda and Contra Costa Counties	52	48

Figure 1. Load position and traffic distribution.

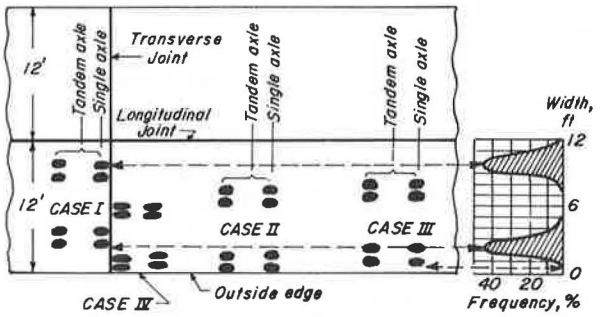

is particularly important in evaluating changes in legal axle-load limits); and

5. Permit a rational approach for the design of overlays for PCC pavements.

LOCATION AND TYPE OF DISTRESS

For a plain jointed PCC pavement, the initial crack (first-stage crack) may be a transverse crack across the middle of the slab or it may be a longitudinal crack that initiates at the transverse joint and propagates in the direction of traffic.

Darter (1) has reported that, based on study of pavements in the American Association of State Highway Officials (AASHO) Test Road and the Michigan Test Road, longitudinal cracking occurred in PCC pavements less than about 8 in in thickness and that transverse cracking occurred in pavements thicker than 8 in.

An analysis of pavements with 8-in-thick concrete layers in the San Francisco Bay area (2) indicated that cracking patterns were dependent on the strength of the cement-stabilized base directly underneath the PCC layer. Two different materials were used: one a cement-treated subgrade (CTS) and the other a cement-treated base (CTB), with CTS being weaker than CTB. The data given in Table 1 indicate that pavements that contain CTS cracked transversely at midslab, while pavements with CTB exhibited considerably more longitudinal cracking. These longitudinal cracks generally started in the inner wheel path of the outer lane at the transverse joint and progressed away from the joint until the slab was completely cracked.

For concrete slab design, a number of locations have been considered for determination of stress. Four such locations are shown in Figure 1 (3).

For case I, stresses at the transverse joint between two adjacent slabs are determined. This location is used as the critical location in both the Portland Cement Association (PCA) (3) and the California Department of Transportation (Caltrans) (4) design procedures. For this situation, the maximum flexural stress is assumed to occur at the underside of the slabs and to act parallel to the transverse joint; this would lead to longitudinal cracking in the wheel path that initiated at the transverse joint edge.

Cases II and III assume that the maximum stress occurs at the pavement lateral edge at midslab length. For both of these cases, Darter (1) concluded from a finite-element analysis that the highest stresses were perpendicular to the transverse joint (i.e., parallel to the longitudinal slab edge) and decreased as the load moved inward. These stresses would lead to transverse cracking in the midpanel position. Distribution of the wheel load across the lane (Figure 1) indicates that case III is probably more critical, since case II occurs only infrequently.

Case IV (corner loading) occurs when the load is located near the transverse and longitudinal joints. This has been neglected in some previous studies because of difficulties in the three-dimensional analysis and the fact that corner cracking is not as common as the longitudinal and transverse cracking for highway-type loading.

STRESS-ANALYSIS PROCEDURES

A number of different procedures are available to estimate stresses and deformations in systems representative of concrete pavement structures. This section briefly summarizes the available methodology, including the procedure selected for this investigation.

Elastic Plate on Dense Liquid Subgrade

Closed-form solutions have been developed for load stresses by Westergaard (5-8) and for temperature-induced stresses by Westergaard (9) and Bradbury (10). Influence charts presented by Pickett and Ray (11) for the load stresses for multiple wheels at various locations in the slab area have been used by PCA (3) and by Caltrans (4), for example, to select slab thicknesses to mitigate fatigue from repetitive traffic loadings for a range in axle loads and for single and tandem axles.

For airfield pavements, PCA (12) and the U.S. Army Corps of Engineers Waterways Experiment Station (USACE-WES) (13) have developed computer solutions for this pavement representation to ascertain stresses (PCA-interior, USACE-WES-edge) for a range in aircraft loads and gear configurations. These programs are currently used for design purposes.

A discrete-element model based on a finite-difference solution (14) has been developed to analyze concrete slabs. The method considers the concrete to be an assemblage of joints, rigid bars, and torsional bars. This analysis is available as a computer program (15).

More recently, finite-element solutions have been developed that can reflect different load-transfer conditions at joints and partial contact between the slab and the dense liquid subgrade (16,17). Computer solutions such as WESLIQUID (18) for stress analysis and JCP (1) for analysis of cumulative damage effects are examples of the methodology.

A major limitation of this pavement representation is that stresses in the materials underlying the concrete cannot be determined. Moreover, it is difficult to assess the influence of the change in stiffness characteristics of materials such as CTB on the response of the concrete to loading.

Elastic Plate on Elastic Foundations

Several solutions have been developed over the years in which the pavement is represented as an elastic

plate resting on an elastic solid [e.g., Hogg (19), Holl (20), Pickett and Ray (11)] or on a layered elastic solid. The finite-element procedure has also been adapted for solution of these situations [Wang and others (21,22) and Huang (23)] and computer solutions are available [e.g., WESLAYER (18)].

Multilayer Elastic Systems

Asphalt concrete pavements have been represented as multilayered elastic solids, and a number of computer programs have been developed to estimate stresses and deformations in such systems, e.g., ELSYM (24), BISAR (25), and CHEVRON, which was developed by H. Warren and W.L. Deickmann in their unpublished report, Numerical Computation of Stresses and Strains in a Multiple-Layer Asphalt Pavement System, which was written for the Chevron Research Corporation in 1963.

Recently, the U.S. Army Corps of Engineers has developed a procedure for concrete pavement design for airfield pavements in which the pavement is expressed as a multilayer elastic solid with full continuity at each of the interfaces (26). This procedure has some disadvantages in that the slab is assumed to be infinite in extent in the horizontal plane. Stresses at the edges have to be increased over those that occur in the interior (the computed stresses) for this analysis procedure.

The finite-element method has some advantage in analyzing this representation in that it has the capability to consider the three-dimensional configurations of concrete slabs. Also, as will be seen, some simplifications can be made to reduce the computational costs associated with finite-element analyses.

Two-Dimensional Finite-Element Models

The applicability of the finite-element solution to pavement problems has been demonstrated in recent years (27-30). Two systems have been used: one an axisymmetric configuration [Figure 2 (27)] and the other a plane strain formulation (Figure 3).

As with the conventional solutions for multilayer elastic systems (e.g., BISAR, ELSYM), the axisymmetric solution is limited, for concrete pavements, to the interior loading condition. The plain strain formulations can be made applicable to determine interior and edge stresses but cannot evaluate corner stresses. An indirect procedure is required in that the interior strip load required to give the same interior stress, as found by axisymmetric or elastic-layer solutions, is determined by trial. This equivalent strip load is then used to calculate edge stresses. Solid SAP (31) and ANSR (32) are representative examples of available computer solutions for two-dimensional problems.

Three-Dimensional Finite-Element Models

One approach to modeling three-dimensional slab configurations is that presented by Wilson and Pretorius (33). It employs a prismatic space finite-element method. The approach is essentially two-dimensional, with the third dimension introduced into the idealization by expressing the load as a Fourier series in this direction. This configuration permits determination of edge but not corner stresses.

The most general method available is the eight-node-brick three-dimensional program (three-dimensional version of Solid SAP). This program permits determination of interior, edge, and corner loadings. It can also accumulate changes in material properties in both the horizontal and the vertical directions.

FINITE-ELEMENT ANALYSES WITH LAYERED ELASTIC SOLID FOUNDATION

Of the analysis methods presented, it was concluded that the finite-element procedure in which the underlying materials are represented as layered elastic solids would be the most appropriate to study the plain jointed concrete pavements used in California.

For this purpose, the Solid SAP three-dimensional program was selected for initial studies. However, time and memory requirements required program modifications. The modifications (2) are based on a procedure used by Otte (34). Symmetry in the x and y directions was used; the concrete slab was divided into four segments, each with a load of P/4 (Figure 4). Superposition of the effects of the fine loads provides the solution. Even with these modifications, the program was very costly to run and required 140 K core memory and central processor time of 8000 s on a CDC 6400 computer.

Figure 5 is a schematic diagram of the loading used. Axle loads of 18 000 lb were used with axle spacings of 7 ft to simulate the principle of tandem axles (in California a 4-ft spacing is more common, but the 7-ft spacing permits the comparison of mid-slab loading and loading at the transverse joint in the same computer analyses).

Two pavement sections on US-101 in the Petaluma area north of San Francisco were analyzed. Each was

Figure 2. Finite-element idealization of a cylinder.

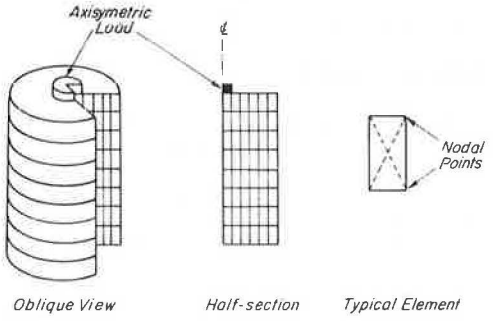

Figure 3. Finite-element idealization of plain strain conditions.

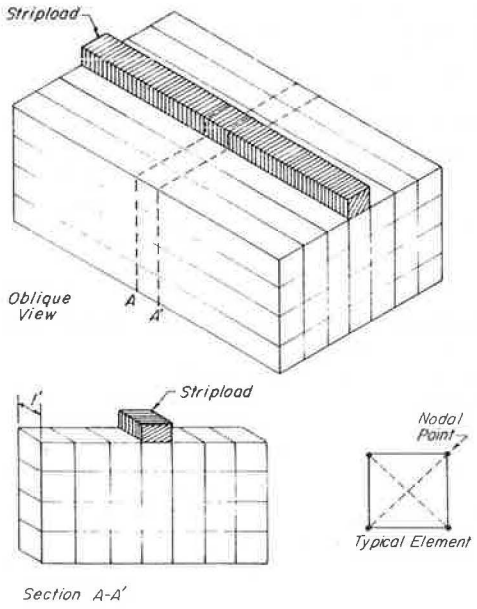

typical of CTS or CTB constructions. Table 2 contains a summary of material properties determined from laboratory tests on recovered samples and from an analysis of construction records. Note that the stiffness characteristics of CTB are about three times that of CTS.

Figures 6, 7, and 8 are plots of S_{xx}, S_{yy}, and the maximum principal stresses for the Petaluma site (pavement with CTS) that used the three-dimensional analysis and assumed no load transfer at the joint. Figure 8 indicates that the maximum stress occurs at the midslab edge, where the principal stress is approximately 10 percent higher than the midslab interior stress. These stresses are larger than the corner stresses and significantly larger than the stresses at the interior wheel at the transverse joint.

It is of interest to note that the S_{xx} stresses are larger than the S_{yy} stresses for the loads located at midslab, which indicates that transverse cracking in the midslab length should be the failure mode. This confirms the observed failure pattern.

Figures 9, 10, and 11 indicate that the Windsor site (pavement with CTB) exhibits much the same stress-distribution patterns, but the stresses are significantly lower in magnitude. Principal stresses at the midslab edge are about 215 psi versus 325 psi at Petaluma. Again, the relative magnitude of the stresses suggests that transverse cracking should be the failure mode. However, the largest value of S_{xx} (180 psi) is only slightly higher than S_{yy} (170 psi). Accordingly, it is possible that, with some load transfer occurring at

Figure 4. Axisymmetric and asymmetric loading conditions.

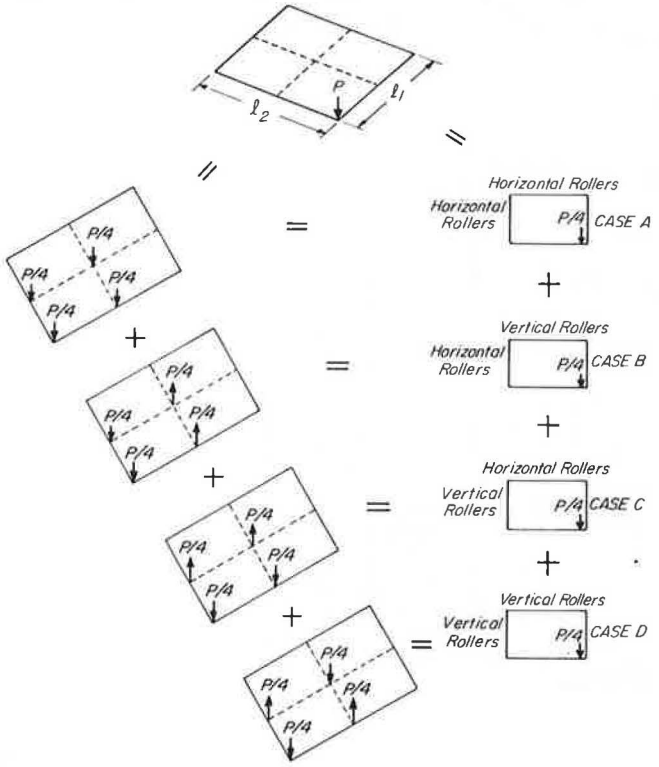

Figure 5. Load positions and stresses considered in fatigue analysis.

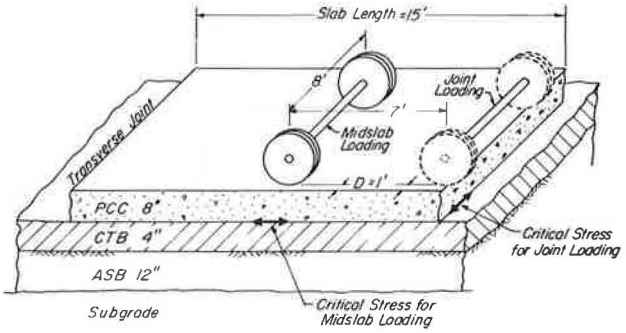

Table 2. Stiffness moduli and layer thicknesses of pavement components.

Component	Stiffness Modulus (psi)		Layer Thickness (in)	
	Windsor (CTB)	Petaluma (CTS)	Windsor (CTB)	Petaluma (CTS)
PCC	4.0×10^6	3.0×10^6	8.0	8.0
Cement-treated layer	1.1×10^6	0.35×10^6	4	4
Aggregate subbase				
Summer	15×10^3	9.0×10^3	12	12
Winter	10×10^3	5.0×10^3		
Subgrade				
Summer	8.0×10^3	7.5×10^3		
Winter	5.0×10^3	4.0×10^3		

Figure 6. S_{xx} stresses on underside of PCC, Petaluma test section.

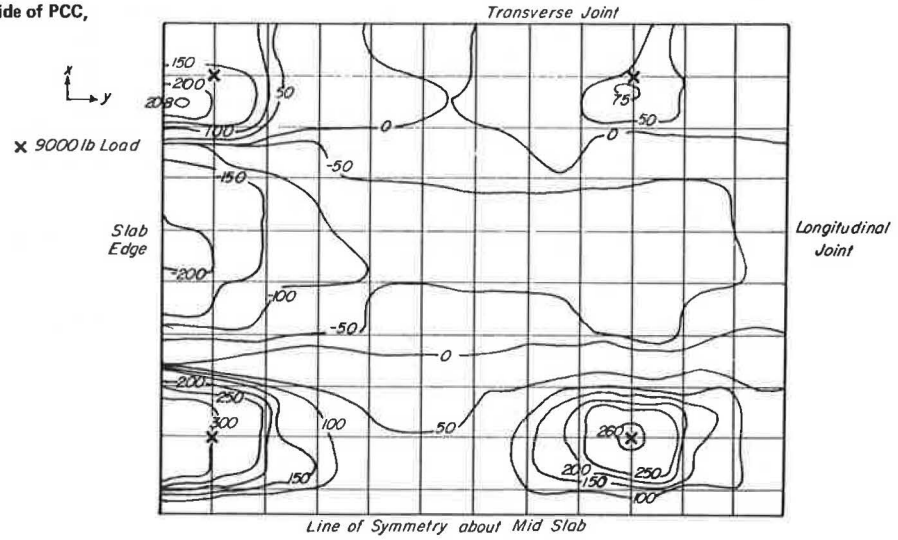

Figure 7. S_{yy} stresses on underside of PCC, Petaluma test section.

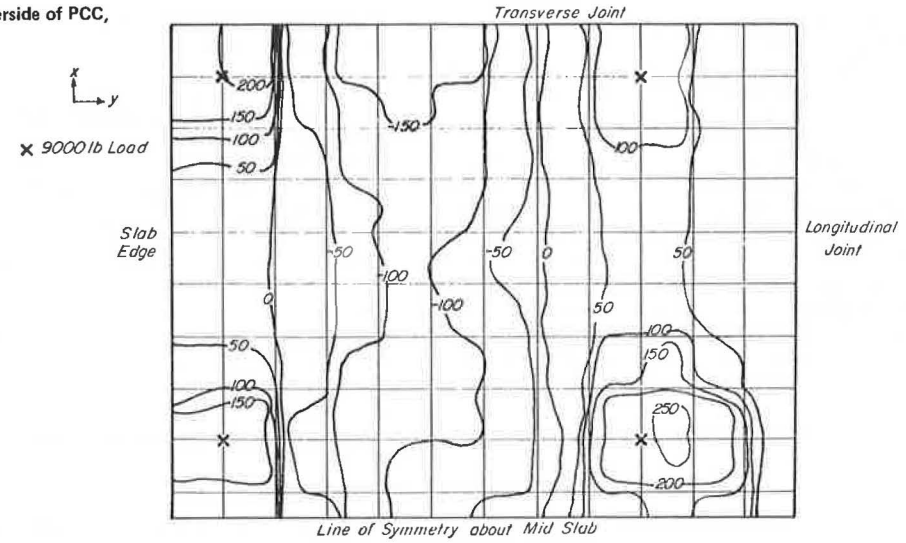

Figure 8. Principal stresses on underside of PCC, Petaluma test section.

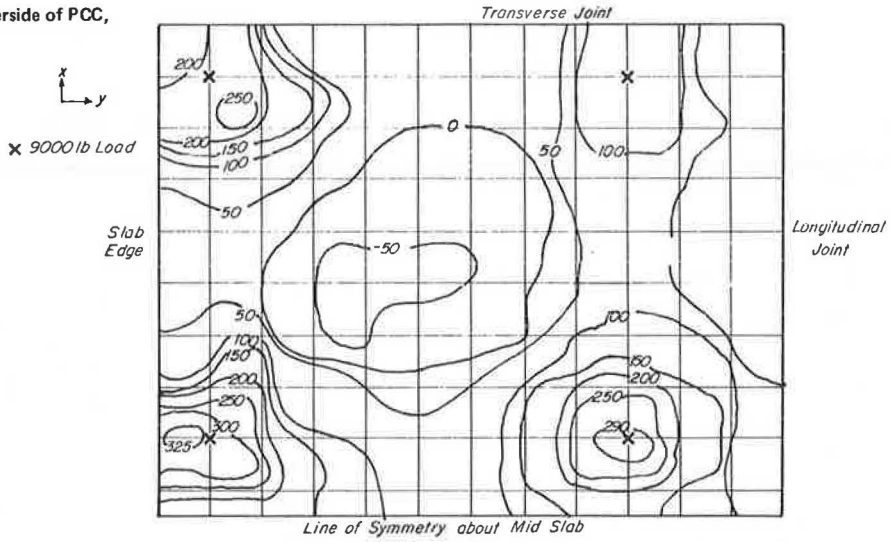

Figure 9. S_{xx} stresses on underside of PCC, Windsor test section.

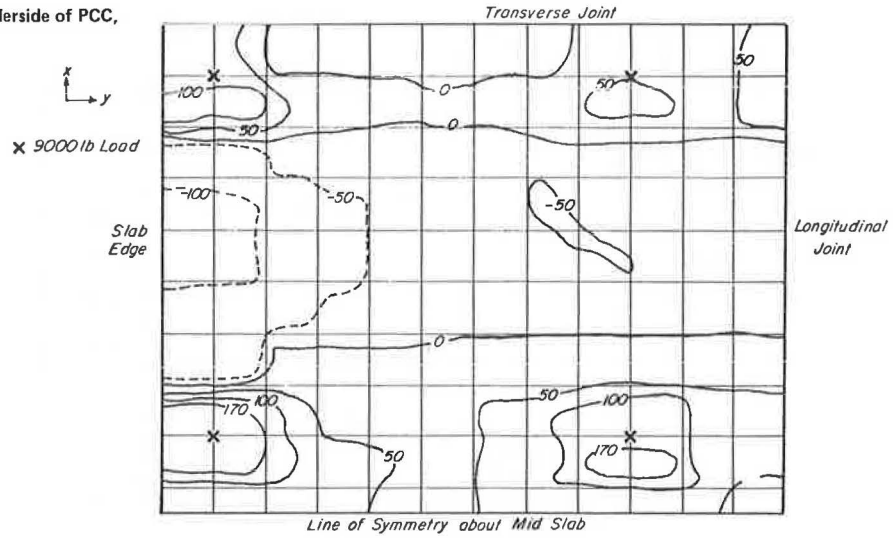

Figure 10. S_{yy} stresses on underside of PCC, Windsor test section.

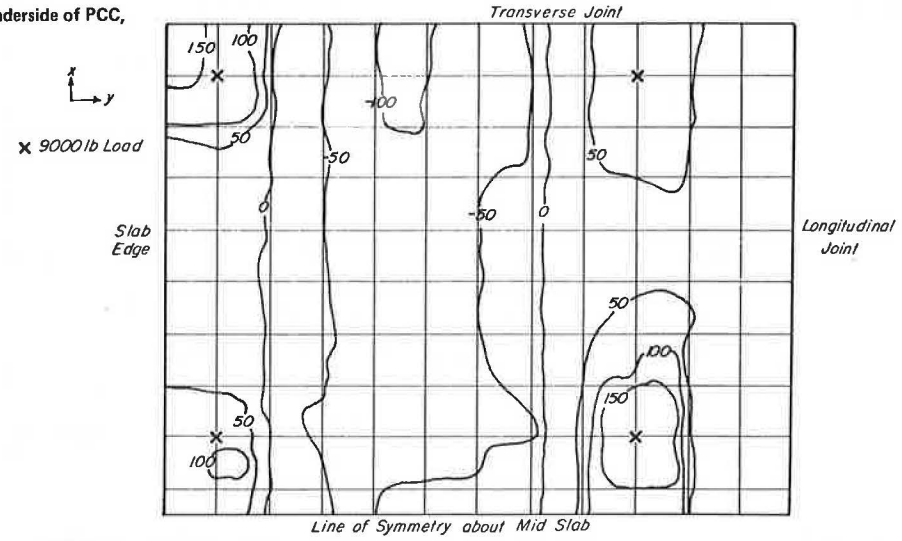

Figure 11. Principal stresses on underside of PCC, Windsor test section.

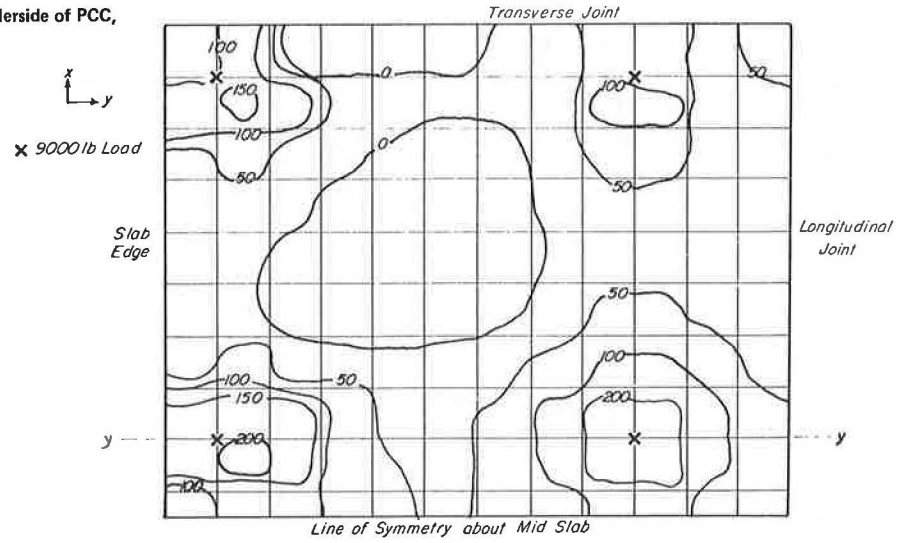

Figure 12. Model used for two-dimensional analysis.

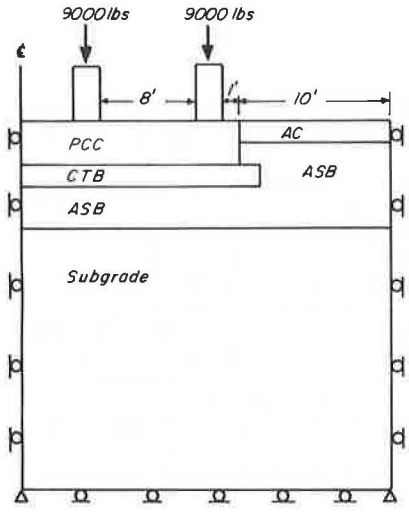

the joints, longitudinal rather than transverse cracking could be obtained and may assist in explaining the observed behavior of more frequent longitudinal cracking with the CTB-type pavements.

The major significance of the three-dimensional analysis is the fact that, in both cases, the maximum principal stresses occur for the midslab loading condition. This suggests that slab response can be analyzed by a simpler two-dimensional finite-element idealization along the y-y axis. Such a situation is representative of stresses caused by an axle at the midslab loading condition or at the transverse joint if full interlock is assumed.

Figure 12 is a schematic diagram of the conditions used for the analyses. Because the two-dimensional model uses a strip load rather than the circular or rectangular loadings employed by the other solutions, it was required to calibrate the solution for the strip load with those obtained for other solutions for the interior loading case where all solutions can be considered equivalent. This was done by adjusting the strip load until it resulted in the same principal stress on the underside of the

Figure 13. Stress distribution for CTB site.

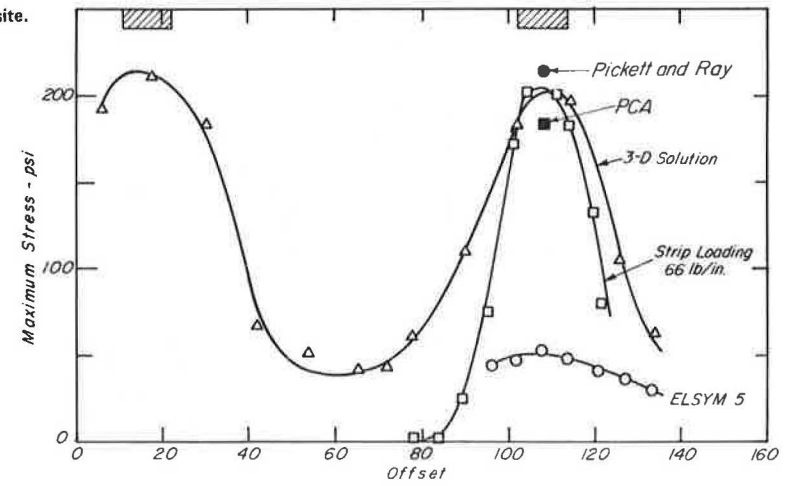

Figure 14. Stress distribution for CTS site.

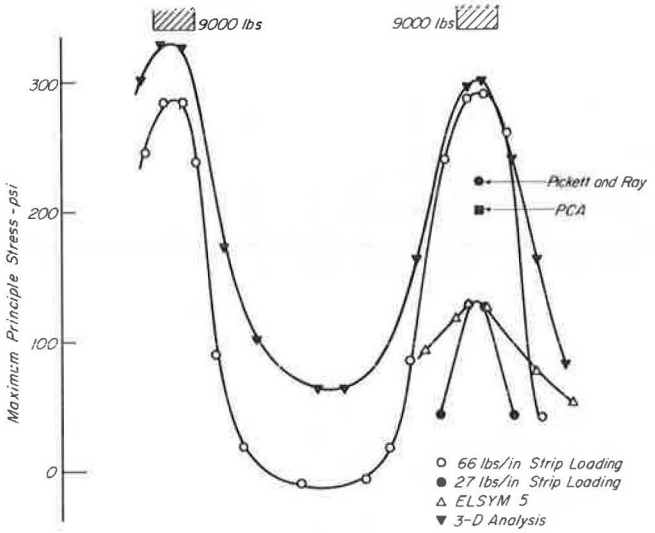

Figure 15. Analysis of pavement components.

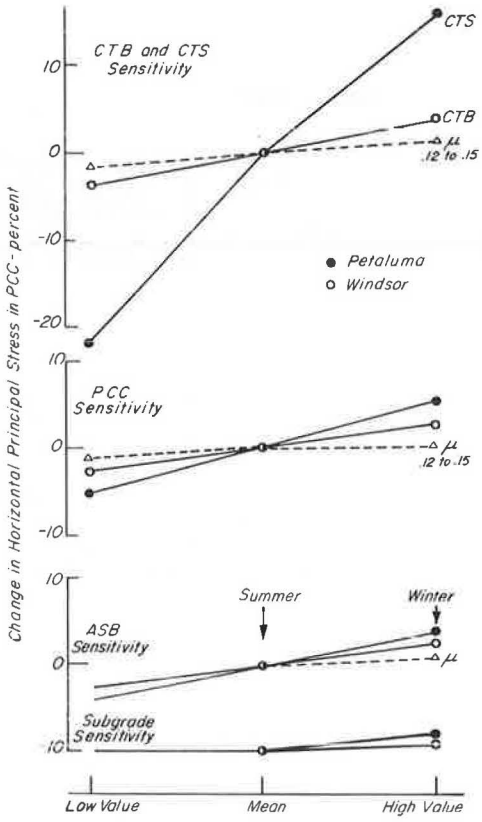

concrete as predicted by the other solutions.

Figures 13 and 14 show the three-dimensional stress distribution and corresponding two-dimensional and ELSYM 5 solutions for the CTB and CTS sites. The strip loading of 66 lb/in agrees with the three-dimensional solution, while a strip loading of 27 lb/in more closely matches the ELSYM 5 solution.

The difference is considerable; the ELSYM 5 solution results in interior stresses of 140 psi while the three-dimensional analysis indicates stresses of 325 psi. There is also a considerable divergence between the three-dimensional and two-dimensional solutions between the loaded wheels. This is not surprising, since previous work with the Solid SAP three-dimensional program (31) indicated that there would be a divergence at lower stresses due to the boundary conditions used. That study indicated, however, that when the stresses were higher, the differences in the calculated stresses would be minimal.

The divergence between the elastic-layer solution was judged significant enough to justify a comparison of estimated stresses by using other procedures [Pickett and Ray (11) influence charts, and the Caltrans (4) method] (k in the range 250 to 300 lb/in^3). The computed values are shown in Figures 13 and 14. For the CTB site (Figure 13), the agreement between three-dimensional Solid SAP, Pickett and Ray, and the PCA method is reasonable, but the elastic-layer solutions (ELSYM and BISAR) indicate much lower stresses.

There is less agreement between solutions for the CTS site, but this is expected, since solutions other than the finite element and elastic layer cannot adequately handle variations in the CTS strength. Comparisons of all solutions indicate that the stresses based on the elastic-layer solutions are too low. Consequently, the two-dimensional strip loadings were adjusted to match the three-dimensional analysis that is believed to be the most accurate. The difference between the elastic-layer solutions (ELSYM 5 and BISAR) and the other solutions remains to be explained.

Results of the two-dimensional finite-element study are summarized in Figure 15 (low value indi-

cates the 10th decile and high values indicate the 90th decile for the stiffness characteristics of the materials analyzed). The steeper the slope of the line in Figure 15, the greater the influence of the parameter on the fatigue life of the pavement. (This is based on the assumption that the horizontal principal stress on the underside of the PCC layer is a determinant of fatigue life.)

Figure 15 indicates that the moduli of the aggregate subbase (ASB) and the subgrade (as well as Poisson's ratio) of these layers have a limited direct influence on the fatigue behavior of the concrete pavement. This is not surprising, since existing design procedures (PCA) have indicated that pavement performance is not changed significantly for minor changes of the modulus of subgrade reaction (k). However, the behavior of the pavement is influenced by the quality of these materials in other than fatigue distress. The better the quality of materials, the better the resistance to pumping, settlement, frost damage, and volume change. This figure does indicate, however, that the expected variations in the CTB have dramatic effects on the performance of the stress level in the concrete layer above it. The results do not imply that the absolute strength of the CTB is more important than the absolute strength of the PCC; it simply indicates that the variations in the strength of CTB that result from a more loosely controlled construction procedure (road mix and acceptance of a wider range of materials) are more significant than the smaller variations in strength of the PCC, which is a more carefully controlled product.

APPLICABILITY OF ANALYSIS TO PREDICT IN-SERVICE PERFORMANCE

To assess the efficacy of this analysis procedure, it was used to predict the performance, as measured by cracking, for both the Windsor and Petaluma sections. In order to do this, it is necessary to simulate the in situ conditions for a range of environmental conditions. In the northern California area in which the pavements are located, the winters are wet and the summers dry. This results in different stiffness moduli for both the untreated subbase and subgrade soils during the year. Table 2 lists representative values for summer and winter conditions.

Daily and monthly variations in temperatures can lead to thermal stresses in the PCC and stabilized bases. When the surface of the PCC is hot and the underside is cooler, this thermal gradient creates tensile stresses on the underside of the PCC. These combine with the load stresses and produce combined tensile stresses on the underside of the pavement. They have a detrimental effect during the hot days and a beneficial effect during the cooler nights.

Thermal stresses can be calculated by using finite-element techniques; however, this study required a more detailed procedure. From weather records, the temperature gradients across the slabs were calculated by using a procedure suggested by Barber (35). The thermal stresses were then determined by the procedure developed by Bradbury (10).

Truck traffic was estimated by the axle group from Caltrans traffic data. This information was further divided into axle weights by using W-4 tables compiled at the weigh stations within the study sections. These data were then classified into five subgroups that represented temperature conditions for noon, midnight, early morning, early evening, and the remaining transition periods. Changes in traffic distribution from month to month were also calculated so that the number of vehicles (n_i) with a given axle weight that had traveled on the particular section of highway could be calculated for each of the applicable thermal conditions.

Because cracking in the PCC is attributable to fatigue, it was necessary to select an appropriate fatigue criterion for the concrete. The relation finally used was that developed by Vesic and Saxena (36):

$$N_f = 225\,000\,(MR/\sigma)^4 \quad (1)$$

where

N_f = number of load applications to failure at stress level σ,
MR = modulus of rupture of concrete, and
σ = tensile stress from traffic load.

Load stresses were combined with the calculated thermal stresses to determine the allowable number of repetitions (N_i) associated with Equation 1. In this instance, since the load stresses are fluctuating and the thermal stresses are constant, it was necessary to use a modified Goodman diagram (30) to determine the allowable number of load repetitions (N_i). Summing the ratios of n_i/N_i for the various subgrade and temperature conditions provides, according to the linear summation of cycle ratios, an indication of the potential for fatigue cracking. The summation should approach unity at failure.

Figure 16 summarizes the cracking data for various segments of the Windsor and Petaluma sections plotted versus n_i/N_i. Note that the procedure is valid for sections that contain both types of cement-stabilized materials.

The same procedure was applied to an additional 1200 lane miles of freeway in various climatic re-

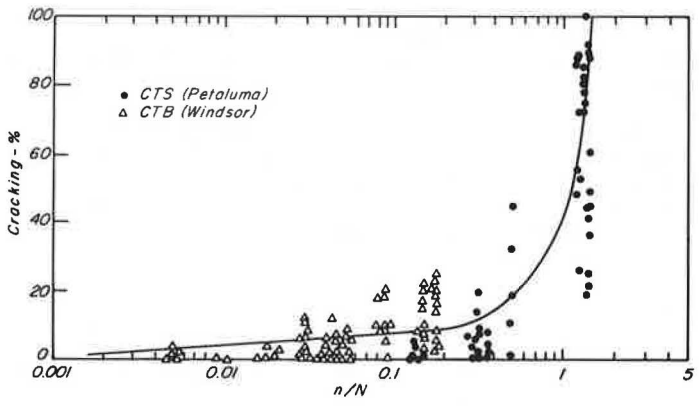

Figure 16. Percentage of total cracking versus n/N, US-101: Marin and Sonoma Counties.

gions of California. The additional analyses supported the validity of the approach (37).

Thus, it would appear that the finite-element procedure, which uses a layered elastic solid rather than the dense liquid subgrade idealization as a representation of the foundation for the PCC, permits a realistic assessment to be made of the influence of properties of the cement-stabilized layer on cracking performance of the concrete.

As an additional consideration, such a procedure is sufficiently general to permit it to be applied to the design of overlays for plain jointed pavements. If the existing concrete slab is not cracked, the thickness of the additional overlay can be determined so that the reduced strains in the existing concrete that result from the overlay will use up the remaining life, which is obtained by subtracting from unity the sum of the n_i/N_i's applied to the time of the overlay.

The finite-element procedure can also be used to examine the development of reflection cracking in the overlay and the use of various treatments to mitigate this phenomenon (38).

CONCLUSIONS

From the material presented in the paper, a few conclusions appear warranted for plain jointed PCC pavements:

1. A two-dimensional finite-element analysis that uses a layered elastic solid rather than a dense liquid subgrade as the idealization of the underlying materials for the concrete layer is suitable for the analysis of the fatigue response. Changes in (a) engineering properties of the foundation materials, (b) loading conditions, and (c) temperature variations can be accommodated.
2. The maximum tensile stress, which is the controlling factor on the fatigue life of this type of pavement, occurs near the edge at the midslab position for the representative highway load configurations examined in the investigation.
3. The finite-element analysis, which permits consideration of different stiffness characteristics of the cement-stabilized layer, has demonstrated that the strength of this layer has a significant influence on the fatigue life of the concrete layer. This analysis has also indicated that different cracking patterns can be identified with different stiffnesses in the cement-stabilized layer.
4. The fatigue relation presented by Vesic and Saxena (36) appears to reasonably predict the cracking performance of the concrete when due consideration is given to the influence of thermal stresses, material variabilities, and traffic repetitions.

ACKNOWLEDGMENT

This study was conducted in cooperation with the Pavement Management System Task Force, Caltrans, and the Federal Highway Administration (FHWA), U.S. Department of Transportation. The contents of this paper reflect our views, and we are responsible for the facts and the accuracy of the data presented herein. The contents do not necessarily reflect the official views or policies of the State of California or FHWA. The paper does not constitute a standard, specification, or regulation.

REFERENCES

1. M.I. Darter. Design of Zero-Maintenance Plain Jointed Concrete Pavement, Vol. 1: Development of Design Procedures. FHWA, Rept. FHWA-RD-77-111, June 1977, 261 pp.
2. D.R. MacLeod. Considerations for Maintenance Strategies for Portland Cement Concrete Pavements. Univ. of California, Berkeley, Ph.D. dissertation, 1979.
3. Thickness Design for Concrete Pavements. Portland Cement Association, Skokie, IL, 1966.
4. Portland Cement Concrete Pavement (7-641). In Highway Design Manual, California Department of Transportation, Sacramento, Dec. 1981.
5. H.M. Westergaard. Computation of Stresses in Concrete Roads. Proc., HRB, Vol. 5, Part I, 1925, pp. 90-112.
6. H.M. Westergaard. Stresses in Concrete Pavements Computed by Theoretical Analysis. Public Roads, Vol. 7, No. 2, April 1926, pp. 25-35.
7. H.M. Westergaard. Stresses in Concrete Runways of Airports. Proc., HRB, Vol. 19, 1939, pp. 197-262.
8. H.M. Westergaard. New Formulas for Stresses in Concrete Pavements of Airfields. Trans., ASCE, Vol. 113, 1948, pp. 425-444.
9. H.M. Westergaard. Analysis of Stresses in Concrete Pavements Due to Variations of Temperature. Proc., HRB, Vol. 6, 1926, pp. 201-215.
10. R.D. Bradbury. Reinforced Concrete Pavements. Wire Reinforcement Institute, Washington, DC, 1938.
11. G. Pickett and G.K. Ray. Influence Charts for Rigid Pavements. Trans., ASCE, Vol. 116, 1951, pp. 49-73.
12. R.G. Packard. Computer Program for Airport Pavement Design (SRO 29.02P). Portland Cement Association, Skokie, IL, 1967.
13. Computerized Aircraft Ground Flotation Analysis, Edge-Loaded Rigid Pavements (H 51). U.S. Army Corps of Engineers Waterways Experiment Station, Vicksburg, MS, 1967.
14. W.R. Hudson and H. Matlock. Analysis of Discontinuous Orthotropic Pavement Slabs Subjected to Combined Loads. HRB, Highway Research Record 131, 1966, pp. 1-48.
15. H.J. Treybig, W.R. Hudson, and A. Abon-Ayyash. Application of Slab Analysis Methods to Rigid Pavement Problems. Center for Highway Research, Univ. of Texas, Austin, Res. Rept. 56-26, May 1972.
16. Y.H. Huang and S.T. Wang. Finite-Element Analysis of Rigid Pavements with Partial Subgrade Contact. TRB, Transportation Research Record 485, 1974, pp. 39-54.
17. A.M. Tabatabaie and E.J. Barenberg. Finite-Element Analysis of Jointed or Cracked Concrete Pavements. TRB, Transportation Research Record 671, 1978, pp. 11-17.
18. Y.T. Chou. Structural Analysis Computer Programs for Rigid Multicomponent Structures with Discontinuities--WESLIQUID and WESLAYER, Report 1: Program Development and Numerical Presentations. U.S. Army Corps of Engineers Waterways Experiment Station, Vicksburg, MS, Tech. Rept. GL-81-6, 1981.
19. A.H.A. Hogg. Equilibrium of a Thin Plate, Symmetrically Loaded, Resting on an Elastic Foundation of Infinite Depth. Philosophical Magazine, Series 7, Vol. 25, 1938, pp. 576-582.
20. D.L. Holl. Thin Plates on Elastic Foundation. In Proc., Fifth International Congress for Applied Mechanics (Cambridge, MA, 1938), Wiley, New York, 1939, pp. 71-74.
21. S.K. Wang, M. Sargious, and Y.K. Cheung. Advanced Analysis of Rigid Pavement. Transportation Engineering Journal, ASCE, Vol. 98, No. TE1, Proc. Paper 8699, Feb. 1972, pp. 37-44.
22. S.K. Wang, M. Sargious, and Y.K. Cheung. Effect of Openings on Stresses in Rigid Pave-

ments. Transportation Engineering Journal, ASCE, Vol. 99, No. TE2, Proc. Paper 9721, May 1973, pp. 255-265.
23. Y.H. Huang. Finite Element Analysis of Slabs on Elastic Solids. Transportation Engineering Journal, ASCE, Vol. 100, No. TE2, May 1974, pp. 403-416.
24. G. Ahlborn. ELSYM Computer Program for Determining Stresses and Deformations in Five Layer Elastic System. Univ. of California, Berkeley, 1972.
25. D.L. DeJong, M.G.F. Peutz, and A.R. Korswagen. Computer Program, BISAR, Layered Systems Under Normal and Tangential Surface Loads. Koninklijke/Shell-Laboratorium, Amsterdam, External Rept. AMSR-0006.73, 1973.
26. F. Parker and others. Development of a Structural Design Procedure for Rigid Airport Pavements. Federal Aviation Administration, Rept. FAA-RD-77-81, 1977.
27. J.M. Duncan, C.L. Monismith, and E.L. Wilson. Finite Element Analysis of Pavements. HRB, Highway Research Record 228, 1968, pp. 11-17.
28. G.L. Dehlen. The Effect of Non-Linear Materials Response on the Behavior of Pavements Subjected to Traffic Loads. Univ. of California, Berkeley, Ph.D. dissertation, 1969.
29. P.E. Fossberg. Load Deformation Characteristics of Three Layer Pavements Containing Cement Treated Base. Univ. of California, Berkeley, Ph.D. dissertation, 1970.
30. P.C. Pretorius. Design Considerations for Pavements Containing Soil-Cement Bases. Univ. of California, Berkeley, Ph.D. dissertation, 1969.
31. E.L. Wilson. Solid SAP: A Static Analysis Program for Three-Dimensional Solid Structures. Univ. of California, Berkeley, Rept. UC-SESM 71-19, 1971.
32. G. Powell and D.P. Monkar. ANSR 1, A General Purpose Program for Analysis of Non-Linear Structural Response. Univ. of California, Berkeley, Rept. EERC-75-37, 1975.
33. E.L. Wilson and P.C. Pretorius. A Computer Program for the Analysis of Prismatic Solids. Univ. of California, Berkeley, Rept. UC-SESM 70-21, 1970.
34. E. Otte. A Structural Design Procedure for Cement Treated Layers in Pavements. Univ. of Pretoria, Pretoria, South Africa, Ph.D. dissertation, 1978.
35. E.S. Barber. Calculation of Maximum Pavement Temperatures from Weather Reports. HRB, Bull. 168, 1957, pp. 1-8.
36. A.S. Vesic and S.K. Saxena. Analysis of Structural Behavior of AASHO Road Test Rigid Pavements. NCHRP, Rept. 97, 1970.
37. D.R. MacLeod and C.L. Monismith. A Cracking Model for Plain Jointed Portland Cement Concrete Pavements. Proc., Second International Conference on Concrete Pavement Design, Purdue Univ., West Lafayette, IN, 1981, pp. 317-330.
38. N.F. Coetzee. Some Considerations on Reflective Cracking for Asphalt Concrete Overlay Pavements. Univ. of California, Berkeley, Ph.D. dissertation, 1979.

Publication of this paper sponsored by Committee on Rigid Pavement Design.

Structural Performance Model and Overlay Design Method for Asphalt Concrete Pavements

A. A. A. MOLENAAR AND CH. A. P. M. VAN GURP

The development of a structural performance model for flexible pavements is described. This model consists of a set of probability-of-survival curves in which the structural deterioration of pavement structures, which are characterized with their equivalent layer thickness, is given with respect to the number of load repetitions. The equivalent layer thickness is calculated according to Odemark's theory. It is shown that the equivalent layer thickness and the survival rate of the pavement can be determined by means of deflection measurements. Furthermore, it is shown how an in situ asphalt concrete fatigue relation can be derived for the construction considered. An overlay design chart based on the equivalent layer thickness concept is given, and an example of how the developed techniques are used for the overlay design of asphalt pavements is presented.

Because the economic recession is restricting the available pavement maintenance and rehabilitation budget, an optimal allocation of this budget for maintenance projects becomes more and more important. It is obvious that, in this situation, engineering judgment alone is not enough to solve overlay design and budget-allocation problems. More emphasis is therefore placed on the so-called rational methods.

This paper describes the efforts of the Laboratory for Road and Railroad Research, Delft University of Technology, on the development of structural performance and overlay design methods. These models are based on deflection measurements that were carried out on several road sections over a three-year period and on a theoretical analysis of three layer pavement systems. An example illustrates the use of these models.

STRUCTURAL PERFORMANCE MODEL: THEORETICAL ANALYSIS

Ninety-three layer structures were analyzed with the BISAR computer program to derive relations between the equivalent layer thickness (h_e) and the maximum strain in the asphalt layer or the vertical compressive strain at the top of the subgrade (1). The equivalent layer thickness is defined as follows:

$$h_e = \sum_{i=1}^{2} 0.9\, h_i \sqrt[3]{E_i/E_3} \quad (1)$$

where

h_e = equivalent layer thickness (m),
h_i = thickness of layer i (m),